Research Square

Preprints are preliminary reports that have not undergone peer review.
They should not be considered conclusive, used to inform clinical practice,
or referenced by the media as validated information.

Prothrombin Complex Concentrate and Fibrinogen Attenuate Doxorubicin-Induced Senescence-Associated Phenotypes in Endothelial Cells

Manni wu
sun yat-sen university
Jiyu Xie
sun yat-sen university
Cheng Lu
Shanghai RAAS Blood Products
Wenli Huang
Shenzhen Weiguang Biological Products (China)
Ya Wang
Chinese Academy of Medical Sciences & Peking Union Medical College
Yang Zhang
zhangy2293@mail.sysu.edu.cn

sun yat-sen university

Article

Keywords: endothelial cells, cellular senescence, doxorubicin, prothrombin complex concentrate, fibrinogen, intravenous immunoglobulin

Posted Date: November 20th, 2026

DOI: https://doi.org/10.21203/rs.3.rs-11518344/v1

License: This work is licensed under a Creative Commons Attribution 4.0 International License.
Read Full License

Additional Declarations: No competing interests reported.

Prothrombin Complex Concentrate and Fibrinogen Attenuate Doxorubicin-Induced Senescence-Associated Phenotypes in Endothelial Cells

Manni Wu[1,†], Jiyu Xie[1,†], Cheng Lu[4], Wenli Huang[5], Ya Wang[3,*], Yang Zhang[1,2,*]

[1] School of Biosafety, Sun Yat-sen University, Shenzhen, Guangdong, China

[2] Guangdong Provincial Key Laboratory of Diabetology, Guangzhou Key Laboratory of Mechanistic and Translational Obesity Research, The Third Affiliated Hospital of Sun Yat-sen University, Guangzhou, Guangdong, China

[3] Institute of Blood Transfusion, Chinese Academy of Medical Sciences & Peking Union Medical College, Chengdu, Sichuan, China

[4] Shanghai RAAS Blood Products Co., Ltd., Shanghai, China

[5] Shenzhen Weiguang Biological Products Co., Ltd., Shenzhen, Guangdong, China

† These authors contributed equally.

* Correspondence:

Yang Zhang
Email: zhangy2293@mail.sysu.edu.cn
Address:
W405, MSC-1, Sun Yat-sen University,
66 Gongchang Rd, Guangming,
Shenzhen, Guangdong, 518012, China

Ya Wang
Email: 175235831@qq.com
Address:
The Institute of Blood Transfusion,
Chinese Academy of Medical Sciences,
26 Hua Cai Rd, Chenghua,
Chengdu, Sichuan, 610052, China.

Abstract

Endothelial senescence and inflammatory activation contribute to vascular injury. Plasma-derived medicinal products may modulate endothelial responses beyond their conventional therapeutic effects, but their activities across different stress conditions remain poorly defined. Human umbilical vein endothelial cells (HUVECs) were exposed to doxorubicin (DOX) or, in separate experiments, tumor necrosis factor α (TNF-α). Human serum albumin (HSA), intravenous immunoglobulin (IVIG), prothrombin complex concentrate (PCC), and fibrinogen (Fg) concentrate were evaluated using senescence-associated β-galactosidase (SA-β-gal) staining, RT-qPCR, immunoblotting, cytokine ELISA, and γH2AX immunofluorescence. Metformin and dexamethasone were included as reference treatments in the DOX and TNF-α experiments, respectively. DOX increased SA-β-gal staining, CDKN1A/p21 expression, and nuclear γH2AX foci. PCC, fibrinogen, and IVIG attenuated several senescence-associated readouts, whereas the effects of HSA were limited. PCC and fibrinogen also reduced γH2AX foci. In TNF-α-stimulated cells, IVIG reduced IL-6 and IL-8 concentrations in the supernatant and attenuated ICAM1, VCAM1, IL6, and IL8 expression. PCC and fibrinogen produced mixed responses, including increased IL-8 under inflammatory stimulation. The endothelial effects of these products depended on the stress model and endpoint. PCC and fibrinogen attenuated DOX-associated senescence markers without broadly suppressing TNF-α-induced inflammation, whereas IVIG showed more consistent anti-inflammatory activity.

Keywords: endothelial cells; cellular senescence; doxorubicin; prothrombin complex concentrate; fibrinogen; intravenous immunoglobulin

Introduction

Population aging is reshaping the landscape of cardiovascular disease. Vascular aging is now recognized as a convergent biological process that increases susceptibility to atherosclerosis, hypertension, heart failure, thrombo-inflammatory syndromes, and treatment-related cardiovascular injury [1]. The endothelium is a highly dynamic monolayer that controls vascular tone, blood fluidity, leukocyte trafficking, permeability, redox balance, and coagulation. Loss of endothelial homeostasis therefore represents an early and mechanistically important event in vascular disease progression [2].

Cellular senescence provides a conceptual framework linking cumulative cellular stress to progressive vascular dysfunction. Senescent endothelial cells undergo stable proliferative arrest and acquire a senescence-associated secretory phenotype (SASP), characterized by increased secretion of inflammatory cytokines, chemokines, growth factors, and matrix-remodeling enzymes [3-5]. In the vascular wall, this secretome can amplify leukocyte recruitment, impair nitric oxide–dependent relaxation, disrupt the endothelial barrier, and propagate paracrine senescence to neighboring cells[2, 6, 7]. Although senescence can serve as a tumor-suppressive and damage-limiting program, persistent endothelial senescence contributes to chronic inflammation, vascular stiffening, plaque instability, and tissue hypoperfusion.

Stress-induced premature senescence (SIPS) is particularly relevant to vascular injury caused by oxidative and genotoxic stress [2]. Doxorubicin is a widely used anthracycline chemotherapeutic, but its clinical utility is limited by cumulative cardiovascular toxicity [8, 9]. Beyond direct cardiomyocyte injury, accumulating evidence indicates that the vascular endothelium is an early target of anthracycline-mediated damage [10, 11]. It can induce reactive oxygen species (ROS) accumulation, topoisomerase-associated DNA damage, activation of the DNA damage response (DDR), p53/p21 signaling, and NF-κB-linked inflammatory programs , thereby providing a robust experimental model for endothelial senescence and chemotherapy-associated vascular dysfunction [12-16]. In HUVECs, nanomolar DOX exposure has been shown to increase SA-β-gal activity, p21 expression, and DNA damage-associated markers; pharmacological studies implicate inflammatory reinforcement through the NLRP3–IL-1β axis [17]. More recently, senescent-cell clearance preserved endothelial vasodilator function in DOX-treated mice, while a senolytic also protected isolated human arterioles during *ex vivo* DOX exposure [18]. Work with the mitochondria-targeted antioxidant MitoQ further connected DOX-associated endothelial senescence to mitochondrial oxidant production and persistent DNA damage signaling [19]. These observations justify examining endothelial stress responses while distinguishing changes in molecular markers from demonstrated recovery of vascular function.

Plasma-derived medicinal products offer a way to investigate how extracellular proteins influence these responses. Albumin solutions can modify endothelial barrier responses to oxidant injury, although their effects depend partly on associated bioactive molecules [20]. HSA contributes to oncotic pressure and ligand transport but also has antioxidant and redox-buffering capacity, particularly through its free thiol chemistry [21]. As a broad immunomodulator, IVIG is capable of dampening endothelial inflammatory activation (e.g., NF-κB-linked responses; leukocyte–

endothelial interactions), conceptually aligned with SASP suppression [22]. IVIG also shows protective effects in vascular injury contexts involving endothelial barrier disruption and leukocyte infiltration, further supporting the notion that immunoglobulin-based products may influence endothelial stress responses [23]. Coagulation factor concentrates, including PCC and fibrinogen, are central to hemostasis and may also influence endothelial signaling through coagulation–inflammation crosstalk, protease-activated receptor (PAR) pathways, and cell-surface interactions [24, 25]. Fibrinogen has also reduced pulmonary endothelial injury in experimental hemorrhagic shock, indicating that its biological effects extend beyond serving as a clotting substrate [26]. These findings provide a rationale for testing clinically used preparations, but they do not establish that the preparations share a common anti-senescence mechanism.

Therefore, in this study, we compared HSA, IVIG, PCC, and fibrinogen concentrate in two separate HUVEC models: DOX-associated senescence phenotypes and TNF-α-induced inflammatory activation. We assessed senescence-associated markers, inflammatory gene expression, supernatant cytokine concentrations, and DNA damage-associated signaling to characterize the responses to each preparation and identify findings that warrant further mechanistic and functional investigation.

Materials and Methods

Cell culture and treatment

Primary human umbilical vein endothelial cells (HUVECs) were obtained from the Cell Resource Center of Peking Union Medical College and used between passages 3 and 6. Cells were maintained at 37°C in a humidified incubator containing 5% CO_2. Complete endothelial cell culture medium consisted of F-12 basal medium (IMMOCELL, IMC-209) supplemented with 10% fetal bovine serum (GIBCO, A5256701), 1% non-essential amino acids(Servicebio, 11140050), insulin(Solarbio, I8830), and 1% penicillin/streptomycin (NCM Biotech, C100C8). Cells were passaged at approximately 80% confluence. Before DOX (MCE, HY-15142) exposure, HUVECs were serum-starved for 12 hours in DMEM (GIBCO, C11995500BT) basal medium containing antibiotics.

Reagents and blood products

The plasma-derived products were supplied by Shanghai RAAS Blood Products Co., Ltd. and Shenzhen Weiguang Biological Products Co., Ltd. Working concentrations were 2 mg/ml HSA, 6.25 mg/ml IVIG, 0.375 IU/mL PCC, and 3.75 mg/ml Fg concentrate. Preparations were diluted in complete culture medium before use.

For assays of senescence-associated phenotypes, HUVECs were exposed to 20 nM DOX for 24 h in the presence or absence of the indicated plasma-derived product. The medium was then replaced with complete culture medium, and cells were allowed to recover for 3 days before RT-qPCR, Western blotting, and γH2AX immunofluorescence analysis, or for 5 days before SA-β-gal staining. Metformin (50 μM, Aladdin, 121369-64-0) was included as a reference treatment. For cytokine measurements, HUVECs were stimulated with TNF-α (25 ng/mL; GLPBIO, GP20964) for 24 h. The stimulation medium was then removed and replaced with

fresh culture medium in the presence or absence of the indicated plasma-derived product. After a further 48 h, culture supernatants were collected for ELISA, and cells were harvested for RT-qPCR analysis. Dexamethasone (SIGMA, D4902) at 1 μM was included as a reference treatment.

Cell viability assay

HUVECs were seeded in 96-well plates at 5 × 10^3 cells per well in 200 μL complete medium. After cell attachment, cells were exposed to increasing concentrations of doxorubicin ranging from 0.02 to 5 μmol/L for 24h . CCK-8 (Sangon Biotech, E606335) reagent was added at 10% of the final volume, and absorbance was measured at 450 nm after incubation at 37°C for 4 hours protected from light. Absorbance was measured at 450 nm using a microplate reader (BioTek SYNERGY H1). CCK-8 was used as a metabolic activity readout during dose selection.

Senescence-associated β-galactosidase staining

Senescence-associated β-galactosidase staining was performed using a commercial kit (Beyotime, RG0039) according to the manufacturer's protocol. Briefly, HUVECs were treated with 20 nM doxorubicin for 24 hours in the presence or absence of HSA, IVIG, PCC, or Fg. The medium was then replaced with complete culture medium, and cells were allowed to recover for 5 days before staining. Cells were fixed and incubated overnight with staining solution at pH 6.0 at 37°C without CO_2. Bright-field images were acquired using a 20× objective (SOPTOP, XD). For each biological replicate, six fields of view were selected by randomly repositioning the microscope stage, avoiding the edges of the well or coverslip. Images were coded and analyzed in ImageJ by an observer blinded to the experimental groups. SA-β-gal-positive cells, identified by blue staining, and total cells were counted. The percentage of SA-β-gal-positive cells was calculated as the number of positive cells divided by the total number of cells. Six independent biological replicates were analyzed, each contributing one value derived from its six fields to the statistical analysis.

RNA extraction and RT-qPCR

Total RNA was extracted from HUVECs using TRIzol reagent (Yeasen, 19211ES60) according to the manufacturer's instructions. RNA concentration and purity were assessed before cDNA synthesis using a reverse-transcription kit (Yeasen, 11142ES60). Quantitative PCR was performed using SYBR Mix (Yeasen, 11184ES08). β-actin (ACTB) was used as the internal control, and relative expression was calculated using the $2^{-\Delta\Delta Ct}$ method. Primer sequences are provided in Table 1.

Western blotting

After treatment, HUVECs were washed with PBS (Servicebio, G4202) and lysed in ice-cold RIPA (Beyotime, P0013B) buffer containing protease and phosphatase inhibitors. Lysates were incubated on ice for 10–15 minutes, collected by scraping, and centrifuged at 14,000 rpm for 10 minutes. Protein concentration was determined using a BCA assay (Beyotime, P0010) . Equal amounts of protein were mixed with 5× loading buffer (Beyotime, P0015L), denatured at 100°C for 10 minutes, separated by 10% SDS-PAGE (Servicebio, G2043), and transferred to PVDF membranes (PALL, BSP0161). Membranes were incubated overnight at 4°C with primary

antibodies against TP53 (1:25000, Proteintech, 21891-1-AP), CDKN1A/p21 (1:2000, Proteintech, 10355-1-AP), and GAPDH (1:25000, Proteintech, 10494-1-AP). HRP-conjugated (1:5000, Proteintech, SA00001-2) secondary antibodies were used for detection, and signals were visualized by enhanced chemiluminescence (MiniChemi910). Uncropped immunoblots are provided as supplemental source data.

γH2AX immunofluorescence

HUVECs grown on 14-mm coverslips were fixed, permeabilized, and incubated overnight with an anti-γH2AX antibody (Beyotime, C2037S), followed by incubation with the corresponding fluorophore-conjugated secondary antibody for 1 hour in the dark. Nuclei were counterstained with DAPI (Servicebio, G1012) for 3–5 minutes. Fluorescent images were captured using a Nikon A1 confocal microscope with a 60× objective. Nuclear γH2AX foci were quantified using Fiji/ImageJ. Six microscopic fields were analyzed for each of six independent biological replicates. The average number of γH2AX foci per nucleus was determined for each biological replicate using images from its six fields, and each replicate contributed one value to the statistical analysis.

ELISA

The concentrations of IL-6(JONLNBIO, JL10208-96T), IL-8(JONLNBIO, JL19291-96T), and total TNF-α(JONLNBIO, JL14113-96T) in cell culture supernatants were measured using commercial ELISA kits (JONLNBIO, Shanghai, China) according to the manufacturer's instructions. Standards and samples were added to antibody-coated 96-well plates, incubated, washed, and developed using HRP-conjugated detection reagent and TMB substrate. Absorbance was measured at 450 nm, and cytokine concentrations were calculated from standard curves. To account for differences in cellular protein content, the measured supernatant concentration was divided by the ratio of total cellular protein in the corresponding sample to that in its control. The resulting protein-normalized concentrations are reported in pg/mL.

Statistical analysis

Data are presented as mean ± SEM unless otherwise indicated. Biological replicates are defined as independent cell-culture experiments performed on different days. Numbers of biological replicates are specified in the corresponding figure legends. Comparisons among multiple groups were performed using one-way analysis of variance followed by Tukey's multiple-comparison test. A two-sided P value <0.05 was considered statistically significant. Statistical analyses were performed using GraphPad Prism version 9.0.

Results

PCC attenuates DOX associated SA β galactosidase staining

We first examined the responses of HUVECs to DOX and the four plasma-derived products. Following exposure to 20nM DOX and a 5-day recovery period, cells showed increased SA-β-gal staining, enlarged and flattened morphology, and lower apparent cell density than untreated controls (Figure 1A). IVIG, PCC, and Fg reduced the percentage of SA-β-gal-positive cells to different extents, with a pronounced

reduction in the PCC group (Figure 1B). Cells treated with PCC or fibrinogen also appeared to retain greater cell density after recovery than cells treated with doxorubicin alone (Figure 1). These findings indicate that plasma-derived products exert differential effects on doxorubicin-induced endothelial senescence phenotypes.

Attenuation of DOX induced senescence and inflammatory gene expression

We next determined whether the phenotypic effects of plasma-derived products were accompanied by changes in senescence-associated and inflammatory gene expression. PCC, fibrinogen, and IVIG significantly attenuated doxorubicin-induced increases in *CDKN1A*, *TP53*, *IL6*, and *IL8* mRNA expression (Figure 2A). In contrast, HSA did not significantly reduce doxorubicin-induced *CDKN1A* or *IL6* expression, although it modestly attenuated the induction of *TP53* and *IL8* (Figure 2A). At the protein level, doxorubicin did not increase total TP53 abundance under these conditions, whereas CDKN1A/p21 was markedly upregulated (Figure 2B & C). The doxorubicin-induced increase in CDKN1A/p21 protein was attenuated by PCC, fibrinogen, and IVIG, but not by HSA (Figure 2B & C). Together, these data suggest that PCC, fibrinogen, and IVIG suppress selected downstream senescence-associated molecular readouts in doxorubicin-treated endothelial cells, with the most consistent effects observed for CDKN1A/p21.

IVIG suppresses TNF α induced inflammatory activation while PCC and Fg produce mixed responses

We next assessed the effects of plasma-derived products on cytokine concentrations in supernatants collected after 48 h of treatment following a 24-h TNF-α prestimulation period and removal of the stimulation medium. TNF-α stimulation significantly increased IL-6 and IL-8 levels in the culture supernatant. Among the four plasma-derived products, IVIG showed the most consistent suppressive effect, significantly reducing TNF-α–induced increases in IL-6 and IL-8 levels. HSA did not significantly alter any of these soluble inflammatory mediators. PCC and Fg did not affect IL-6 release but further increased IL-8 levels under TNF-α–stimulated conditions (Figure 3A).

At the transcript level, TNF-α significantly increased the expression of *ICAM1*, *VCAM1*, *IL6*, and *IL8*. IVIG attenuated the induction of all four inflammatory transcripts. HSA selectively increased *VCAM1* expression without significantly altering *ICAM1*, *IL6*, or *IL8*. PCC reduced TNF-α–induced *ICAM1* and *VCAM1* expression but further increased *IL8* expression. Fg increased the expression of *VCAM1*, *IL6*, and *IL8* under TNF-α stimulation. As expected, dexamethasone suppressed the TNF-α–induced expression of selected inflammatory markers (Figure 3B). Together, the IL-6/IL-8 and transcript measurements support a broadly suppressive effect of IVIG in this model, whereas the responses to PCC and Fg depended on the endpoint.

PCC and Fg reduce nuclear γH2AX foci after DOX exposure

We further examined whether plasma-derived products altered DNA damage response–associated signaling in doxorubicin-treated HUVECs. Doxorubicin increased nuclear γH2AX foci formation, consistent with activation of DNA damage–associated signaling (Figure 4). PCC and fibrinogen significantly reduced the average number of γH2AX foci per nucleus, whereas HSA and IVIG showed weaker

or less consistent effects. These observations associate the PCC and Fg responses with reduced DNA damage-associated signaling.

Discussion

This study compared the effects of four plasma-derived preparations on DOX-associated senescence phenotypes and TNF-α-induced inflammatory activation in HUVECs. PCC, fibrinogen, and IVIG attenuated selected DOX-associated senescence markers, whereas HSA showed limited effects. PCC and fibrinogen also reduced γH2AX foci. In the separate TNF-α model, IVIG consistently suppressed inflammatory responses, whereas PCC and fibrinogen enhanced selected inflammatory endpoints. These findings reveal distinct effects of clinically used plasma-derived preparations on endothelial stress responses and identify PCC and fibrinogen as candidates for further investigation of DOX-associated senescence phenotypes. More broadly, they provide a rationale for exploring defined plasma-derived preparations as potential senotherapeutic agents within the emerging framework of blood-based systemic rejuvenation [27, 28].

The attenuation of DOX-associated senescence markers by PCC and fibrinogen is notable in the context of bidirectional interactions between coagulation-related signaling and cellular senescence. Wiley et al. identified increased secretion of hemostasis-related proteins by senescent fibroblasts and showed that senescent-cell clearance attenuated DOX-associated increases in blood clotting in mice [29]. Conversely, thrombin induced senescence in porcine atrial endothelial cells through pathways involving oxidative stress and activation of the local angiotensin system [30]. More recent studies identified thrombomodulin (THBD)–PAR1 signaling as a pathway supporting senescent-cell survival, with PAR1 inhibition by vorapaxar reducing senescent-cell accumulation and ameliorating experimental liver fibrosis [31-33]. These findings highlight the importance of coagulation-related signaling in senescence, while indicating that its consequences depend on the cellular context. The responses observed here therefore warrant examination of the composition and signaling properties of these preparations beyond their hemostatic functions. For PCC, one testable possibility is a contribution from protein C, if present in the preparation and activated under the culture conditions. Activated protein C (APC) can suppress TNF-α-induced endothelial *VCAM-1* expression through signaling involving PAR1, S1PR1, and GRK2 [34]. However, thrombomodulin and endothelial protein C receptor (EPCR) influence PAR1 cleavage and determine the signaling responses to thrombin and APC [25]. Moreover, protein C activation also participates in the THBD-dependent pathway that supports senescent-cell survival, indicating that cytoprotection does not necessarily imply suppression of senescence [32]. Thus, the involvement of APC–PAR1 signaling in the PCC response remains a hypothesis requiring characterization of the preparation and direct pathway perturbation. Fibrinogen may influence endothelial injury through distinct processes: in mice subjected to hemorrhagic shock, fibrinogen resuscitation restored pulmonary syndecan-1 mRNA levels and reduced lung permeability [26]. Nevertheless, both PCC and fibrinogen increased IL-8 concentrations under TNF-α stimulation. Their attenuation of DOX-associated senescence markers should therefore be interpreted

alongside these inflammatory responses when assessing their overall effects on the endothelium.

The anti-inflammatory effect of IVIG observed in our study is consistent with its established immunomodulatory properties and provides a rationale for investigating its potential senomorphic activity through modulation of the senescence-associated secretory phenotype (SASP) [6, 35]. In an endothelialized model of heparin-induced thrombocytopenia, IVIG pretreatment of whole blood reduced cellular adhesion and thrombus formation over TNF-α-activated HUVECs [36]. Although that system incorporates pathogenic antibodies and circulating cells, our findings demonstrate modulation of inflammatory responses in endothelial monoculture. Several mechanisms may contribute to these effects. Das et al. showed that IVIG suppresses inflammatory cytokine production in innate immune cells through autophagy, with this response depending on $F(ab')_2$ fragments and IgG internalization but not on sialylation [37]. More recently, Jones et al. showed that Fc-engineered, sialylated IgG1 Fc constructs with enhanced affinity for FcγRIIB had greater anti-inflammatory potency than IVIG in mouse models of autoimmunity [38]. These studies identify autophagy and immunoglobulin–receptor interactions as candidate mechanisms for the endothelial effects of IVIG, although their involvement remains untested. IVIG also reduced *IL6* and *IL8* expression after DOX exposure, suggesting an effect on senescence-associated inflammatory transcription. However, SASP secretion was not assessed following treatment of established senescent cells, so these findings do not establish senomorphic activity. Testing IVIG and engineered, sialylated IgG1 Fc constructs in this setting, with matched wild-type sialylated Fc controls and measurements of SASP secretion, viability, and paracrine activity, would clarify their effects on senescence-associated inflammation.

Although HSA showed limited effects on DOX-associated senescence markers in our model, its activity should be considered in relation to its molecular state and associated ligands. Albumin contributes to extracellular antioxidant defense through its Cys34 thiol, whose reactivity and antioxidant properties are influenced by fatty acid binding and glycation [39-41]. These properties may help explain why different albumin preparations produce different biological responses. In a microfluidic model of endothelial oxidant injury, Diebel et al. found that the protection provided by albumin solutions varied with their sphingosine-1-phosphate content [20]. Sulfhydrated bovine serum albumin also reduced LPS-induced macrophage adhesion to endothelial cells and ameliorated DOX-induced cardiac and intestinal injury in mice, supporting a role for albumin thiol modifications in its protective effects [42]. Conversely, AGE-modified HSA increased SA-β-gal expression in human coronary artery endothelial cells [43]. Together, these studies suggest that albumin's endothelial effects depend on its chemical modifications and bound molecules, as well as the experimental setting. Our preparation was not characterized for oxidation, glycation, or lipid cargo, precluding attribution of its limited activity to any of these properties. The present findings therefore apply to the preparation and concentration tested. Comparisons of albumin preparations with defined redox states and ligand content would help determine whether these features influence endothelial responses to DOX.

Our comparison of individual plasma-derived preparations complements studies investigating how changes in the circulating milieu influence aging. Small extracellular vesicles isolated from young mouse plasma improved mitochondrial function and several age-associated phenotypes in aged mice, demonstrating that biologically active plasma constituents extend beyond soluble proteins [44]. A small human study also reported changes in epigenetic age estimates and other molecular biomarkers following therapeutic plasma exchange, including regimens supplemented with IVIG [45]. However, that intervention combined plasma removal with albumin replacement, with or without IVIG, and therefore does not establish the effects of administering individual products alone or demonstrate clinical rejuvenation. Testing individual preparations under defined conditions may help clarify their endothelial effects, although interactions among plasma constituents and their consequences *in vivo* remain unresolved [46].

Several limitations affect the interpretation of these findings. HUVEC monocultures model selected endothelial responses to stress but do not reproduce adult vascular aging or interactions with circulating cells and other tissues. Testing each preparation at a single concentration also limits assessment of dose dependence and does not establish comparative potency or effective exposure *in vivo*. Moreover, the products were administered during DOX exposure; the findings therefore concern modulation of the developing senescence-associated phenotype and do not establish reversal of pre-existing senescence. Reductions in SA-β-gal staining, p21 expression, and γH2AX foci do not by themselves demonstrate durable restoration of endothelial function or enhanced DNA repair. Finally, the active constituents and signaling pathways responsible for the observed responses remain unresolved.

Further work should prioritize dose–response studies and treatment initiated after senescence has developed, with assessment of viability, sustained proliferative arrest, secreted SASP factors, and endothelial barrier and vasodilator function. Characterizing product composition and testing individual constituents, followed by targeted perturbation of candidate receptors and pathways, would help distinguish specific signaling effects from broader changes in cellular stress or DOX exposure. Validation in adult endothelial cells and appropriate animal models should precede consideration of clinical studies. For PCC and fibrinogen, any vascular benefit would need to be evaluated alongside coagulation activation and thrombotic outcomes. Combinations with IVIG could also be examined, but complementary activity should be demonstrated experimentally, particularly given the increases in selected inflammatory endpoints observed with PCC and fibrinogen.

In conclusion, clinically used plasma-derived preparations exert distinct effects on endothelial stress responses in vitro. PCC and fibrinogen attenuated DOX-associated senescence markers, whereas IVIG more consistently suppressed TNF-α-induced inflammatory activation. These findings provide a basis for investigating how individual preparations influence endothelial injury and senescence, with mechanistic and functional validation needed to determine their therapeutic relevance.

Data Availability

The data generated and analysed during the current study are available from the corresponding authors on reasonable request.

References

1. Ungvari, Z., Tarantini, S., Donato, A. J., Galvan, V. & Csiszar, A. Mechanisms of vascular aging. *Circ. Res.* **123,** 849–867 (2018).
2. López-Otín, C., Blasco, M. A., Partridge, L., Serrano, M. & Kroemer, G. Hallmarks of aging: An expanding universe. *Cell* **186,** 243–278 (2023).
3. Coppé, J. P., Desprez, P. Y., Krtolica, A. & Campisi, J. The senescence-associated secretory phenotype: the dark side of tumor suppression. *Annu. Rev. Pathol.* **5,** 99–118 (2010).
4. Minamino, T. et al. Endothelial cell senescence in human atherosclerosis: role of telomere in endothelial dysfunction. *Circulation* **105,** 1541–1544 (2002).
5. Han, Y. & Kim, S. Y. Endothelial senescence in vascular diseases: current understanding and future opportunities in senotherapeutics. *Exp. Mol. Med.* **55,** 1–12 (2023).
6. Wang, B., Han, J., Elisseeff, J. H. & Demaria, M. The senescence-associated secretory phenotype and its physiological and pathological implications. *Nat. Rev. Mol. Cell Biol.* **25,** 958–978 (2024).
7. Najari Beidokhti, M. et al. Lung endothelial cell senescence impairs barrier function and promotes neutrophil adhesion and migration. *GeroScience* **47,** 2655–2671 (2025).
8. Herrmann, J. et al. Vascular toxicities of cancer therapies: the old and the new--an evolving avenue. *Circulation* **133,** 1272–1289 (2016).
9. Koene, R. J., Prizment, A. E., Blaes, A. & Konety, S. H. Shared risk factors in cardiovascular disease and cancer. *Circulation* **133,** 1104–1114 (2016).
10. Spallarossa, P. et al. Doxorubicin induces senescence or apoptosis in rat neonatal cardiomyocytes by regulating the expression levels of the telomere binding factors 1 and 2. *Am. J. Physiol. Heart Circ. Physiol.* **297,** H2169–H2181 (2009).
11. He, H. et al. Doxorubicin induces endotheliotoxicity and mitochondrial dysfunction via ROS/eNOS/NO pathway. *Front. Pharmacol.* **10,** 1531 (2019).
12. Abdelgawad, I. Y., Agostinucci, K. & Zordoky, B. N. Cardiovascular ramifications of therapy-induced endothelial cell senescence in cancer survivors. *Biochim. Biophys. Acta Mol. Basis Dis.* **1868,** 166352 (2022).
13. Cappetta, D. et al. Oxidative stress and cellular response to doxorubicin: a common factor in the complex milieu of anthracycline cardiotoxicity. *Oxid. Med. Cell Longev.* **2017,** 1521020 (2017).
14. Kurz, D. J., Decary, S., Hong, Y. & Erusalimsky, J. D. Senescence-associated (beta)-galactosidase reflects an increase in lysosomal mass during replicative ageing of human endothelial cells. *J. Cell Sci.* **113,** 3613–3622 (2000).
15. Donato, A. J., Morgan, R. G., Walker, A. E. & Lesniewski, L. A. Cellular and molecular biology of aging endothelial cells. *J. Mol. Cell Cardiol.* **89,** 122–135 (2015).
16. Wang, S. et al. Doxorubicin induces apoptosis in normal and tumor cells via distinctly different mechanisms. intermediacy of H(2)O(2)- and p53-dependent pathways. *J. Biol. Chem.* **279,** 25535–25543 (2004).
17. Shamoon, L. et al. Resolvin E1 attenuates doxorubicin-induced endothelial senescence by modulating NLRP3 inflammasome activation. *Biochem. Pharmacol.* **201,** 115078 (2022).
18. Venkatasubramanian, R. et al. Cellular senescence mediates doxorubicin chemotherapy-induced vascular endothelial dysfunction: translational

evidence of prevention with senolytic treatment. *Am. J. Physiol. Heart Circ. Physiol.* **329,** H1672–H1683 (2025).
19. Abdeahad, H. et al. MitoQ reduces senescence burden in doxorubicin-treated endothelial cells by reducing mitochondrial ROS and DNA damage. *Am. J. Physiol. Heart Circ. Physiol.* **329,** H1154–H1161 (2025).
20. Diebel, L. N., Liberati, D. M. & Carge, M. Effect of albumin solutions on endothelial oxidant injury: A microfluidic study. *Surgery* **173,** 876–882 (2023).
21. Taverna, M., Marie, A. L., Mira, J. P. & Guidet, B. Specific antioxidant properties of human serum albumin. *Ann. Intensive Care* **3,** 4 (2013).
22. Wiatr, M. et al. Anti-inflammatory activity of intravenous immunoglobulin through scavenging of heme. *Mol. Immunol.* **111,** 205–208 (2019).
23. Widiapradja, A. et al. Intravenous immunoglobulin (IVIg) provides protection against endothelial cell dysfunction and death in ischemic stroke. *Exp. Transl. Stroke Med.* **6,** 7 (2014).
24. Rezaie, A. R. Protease-activated receptor signalling by coagulation proteases in endothelial cells. *Thromb. Haemost.* **112,** 876–882 (2014).
25. Biswas, I., Giri, H., Panicker, S. R. & Rezaie, A. R. Thrombomodulin switches signaling and protease-activated receptor 1 cleavage specificity of thrombin. *Arterioscler. Thromb. Vasc. Biol.* **44,** 603–616 (2024).
26. Chipman, A. M., Wu, F. & Kozar, R. A. Fibrinogen inhibits microRNA-19b, a novel mechanism for repair of haemorrhagic shock-induced endothelial cell dysfunction. *Blood Transfus.* **19,** 420–427 (2021).
27. Liu, M.-N., Lan, Q., Wu, H. & Qiu, C.-W. Rejuvenation of young blood on aging organs: effects, circulating factors, and mechanisms. *Heliyon* **10,** e32652 (2024).
28. Bieri, G., Schroer, A. B. & Villeda, S. A. Blood-to-brain communication in aging and rejuvenation. *Nat. Neurosci.* **26,** 379–393 (2023).
29. Wiley, C. D. et al. SILAC analysis reveals increased secretion of hemostasis-related factors by senescent cells. *Cell Rep.* **28,** 3329–3337.e5 (2019).
30. Hasan, H. et al. Thrombin induces angiotensin II-mediated senescence in atrial endothelial cells: impact on pro-remodeling patterns. *J. Clin. Med.* **8,** 1570 (2019).
31. Webster, C. M. & van Deursen, J. M. Senolysis through thrombomodulation. *Cell Res.* **33,** 575–576 (2023).
32. Maeso-Díaz, R. et al. Targeting senescent hepatocytes using the thrombomodulin-PAR1 inhibitor vorapaxar ameliorates NAFLD progression. *Hepatology* **78,** 1209–1222 (2023).
33. Pan, C. C. et al. Antagonizing the irreversible thrombomodulin-initiated proteolytic signaling alleviates age-related liver fibrosis via senescent cell killing. *Cell Res.* **33,** 516–532 (2023).
34. Birch, C. A. et al. Endothelial APC/PAR1 distinctly regulates cytokine-induced pro-inflammatory VCAM-1 expression. *Front. Mol. Biosci.* **10,** 1211597 (2023).
35. Sahu, P. & Satapathy, T. Immunopharmacology of senescence: targeting the senescence-associated secretory phenotype (SASP)—a mechanism-based review. *Inflammopharmacology* **33,** 4291–4310 (2025).
36. Witzemann, A. et al. Intravenous immunoglobulin prevents thrombosis in an endothelialized disease model of heparin-induced thrombocytopenia. *J. Thromb. Haemost.* **23,** 1657–1666 (2025).
37. Das, M. et al. Intravenous immunoglobulin mediates anti-inflammatory effects in peripheral blood mononuclear cells by inducing autophagy. *Cell Death Dis.* **11,** 50 (2020).
38. Jones, A. T., Marino, A. E., Martynyuk, T., Bournazos, S. & Ravetch, J. V. The anti-inflammatory activity of IgG is enhanced by co-engagement of type I and II Fc receptors. *Science* **390,** eadv2927 (2025).

39. Uzelac, T. et al. The thiol group reactivity and the antioxidant property of human serum albumin are controlled by the joint action of fatty acids and glucose binding. *Int. J. Mol. Sci.* **25,** 2335 (2024).
40. Belinskaia, D. A., Voronina, P. A., Shmurak, V. I., Jenkins, R. O. & Goncharov, N. V. Serum albumin in health and disease: esterase, antioxidant, transporting and signaling properties. *Int. J. Mol. Sci.* **22,** 10318 (2021).
41. Jala, A., Tayyari, F. & Funk, W. E. Use of human serum albumin Cys34 (HSA-Cys34) adductomics as a multidimensional and integrative biomarker approach to assess oxidative stress. *Antioxidants* **15,** 458 (2026).
42. Xu, Y. et al. Sulfhydrated albumin transmits H(2)S signaling and ameliorates DOX-induced multiorgan injuries. *Redox Biol.* **83,** 103631 (2025).
43. Shen, C.-Y. et al. Unveiling the molecular basis of inflamm-aging induced by advanced glycation end products (AGEs)-modified human serum albumin (AGE-HSA) in patients with different immune-mediated diseases. *Clin. Immunol.* **252,** 109655 (2023).
44. Chen, X. et al. Small extracellular vesicles from young plasma reverse age-related functional declines by improving mitochondrial energy metabolism. *Nat. Aging* **4,** 814–838 (2024).
45. Fuentealba, M. et al. Multi-omics analysis reveals biomarkers that contribute to biological age rejuvenation in response to single-blinded randomized placebo-controlled therapeutic plasma exchange. *Aging Cell* **24,** e70103 (2025).
46. Gulej, R. et al. Plasma-based strategies for systemic rejuvenation: critical perspectives on clinical translation. *GeroScience* **48,** 4571–4584 (2026).

Acknowledgements

This work was supported by Basic Research Fund in Shenzhen Natural Science Foundation (JCYJ20250604174404006) and Shenzhen Medical Research Fund (B2502034) (YZ).

Author contributions

MW, JX: methodology, investigation, visualization, writing-original draft; CL, WH: writing-review and editing; YZ, YW: conceptualization, methodology, investigation, visualization, project administration, data curation, supervision, writing-review and editing. All authors have read and agreed to the published version of the manuscript.

Additional Information

Competing interests

Cheng Lu and Wenli Huang are affiliated with Shanghai RAAS Blood Products Co., Ltd. and Shenzhen Weiguang Biological Products Co., Ltd., respectively. These authors facilitated the provision of plasma-derived products from their respective companies and contributed to manuscript writing and review. The remaining authors declare no competing interests.

Figure Legends

Figure 1. Plasma-derived products differentially attenuate doxorubicin-induced senescence-associated β-galactosidase activity in HUVECs. (A) Representative bright-field images of SA-β-gal staining in HUVECs treated with doxorubicin (Dox, 20 nM) for 24 hours in the absence or presence of human serum albumin (HSA, 2 mg/ml), intravenous immunoglobulin (IVIG, 6.25 mg/ml), prothrombin complex concentrate (PCC,0.375 IU/ml), or fibrinogen concentrate (Fg, 3.75 mg/ml). Metformin (Met,50 μM) was included as a comparator as indicated. SA-β-gal–positive cells are shown in blue. Scale bar, 100 μm. (B) Quantification of SA-β-gal-positive cells, expressed as a percentage of the total number of cells. Data are presented as mean ± SEM from six independent biological replicates, with six microscopic fields analyzed per replicate. Each biological replicate contributed one value to the statistical analysis. Statistical analysis was performed using one-way ANOVA followed by Tukey's multiple-comparison test. P values for significant pairwise comparisons are indicated in the figure.

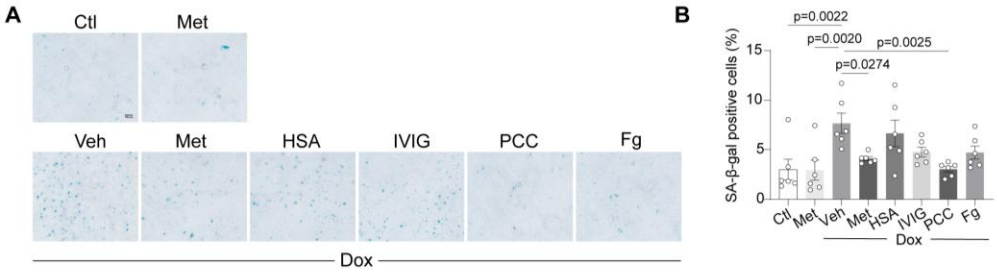
Figure 2. Plasma-derived products modulate doxorubicin-induced senescence-associated and SASP-related molecular readouts in HUVECs. (A) Relative mRNA expression of senescence-associated genes *CDKN1A* and *TP53* and SASP-related inflammatory genes *IL6* and *IL8* in HUVECs treated with doxorubicin (Dox, 20nM) in the absence or presence of four plasma-derived products. Gene expression was normalized to β-actin and expressed relative to the control group. (B) Representative Western blots showing TP53 and CDKN1A/p21 protein abundance. GAPDH was used as the loading control. (C) Densitometric quantification of TP53 and CDKN1A/p21 protein abundance normalized to GAPDH. Data are presented as mean ± SEM. For qRT-PCR (A), each point represents the mean of four biological replicates from one of three independent experiments; error bars indicate the SEM of the three experimental means. All biological replicate values (n = 12 per group) were analyzed using one-way ANOVA followed by Tukey's multiple comparisons test, with comparisons against the DOX-only group (Veh). Veh denotes the DOX-only group. Western blot data (C; n = 3 independent biological replicates) were analyzed using one-way ANOVA followed by Tukey's multiple comparisons test. Adjusted P values for significant comparisons are indicated in the figure.

Figure 3. IVIG consistently suppresses TNF-α–induced endothelial inflammatory activation, whereas PCC and fibrinogen exert endpoint-specific effects.(A) Concentrations of IL-6, IL-8, and total TNF-α in culture supernatants. HUVECs were stimulated with TNF-α (25 ng/mL) for 24 h, after which the stimulation medium was removed and replaced with fresh culture medium in the absence or presence of HSA (2 mg/ml), IVIG (6.25 mg/ml), PCC (0.375 IU/mL), or Fg (3.75 mg/ml). Supernatants were collected after a further 48 h and analyzed by ELISA. Cytokine concentrations were measured by ELISA and normalized by dividing the measured concentration by the ratio of sample cellular protein content to that of the corresponding control. Protein-normalized concentrations are expressed in pg/mL. Dexamethasone (1 μM) was included as an anti-inflammatory comparator as indicated. (B) Relative mRNA expression of inflammatory and adhesion-related genes *ICAM1*, *VCAM1*, *IL6*, and *IL8*. Gene expression was normalized to β-actin and expressed relative to the control group. Data are presented as mean ± SEM; n=4 independent biological replicates for

ELISA and n=3 independent biological replicates for quantitative reverse transcription PCR. Statistical analysis was performed by 1-way ANOVA followed by Tukey multiple-comparison test. P values for significant pairwise comparisons are indicated in the figure.

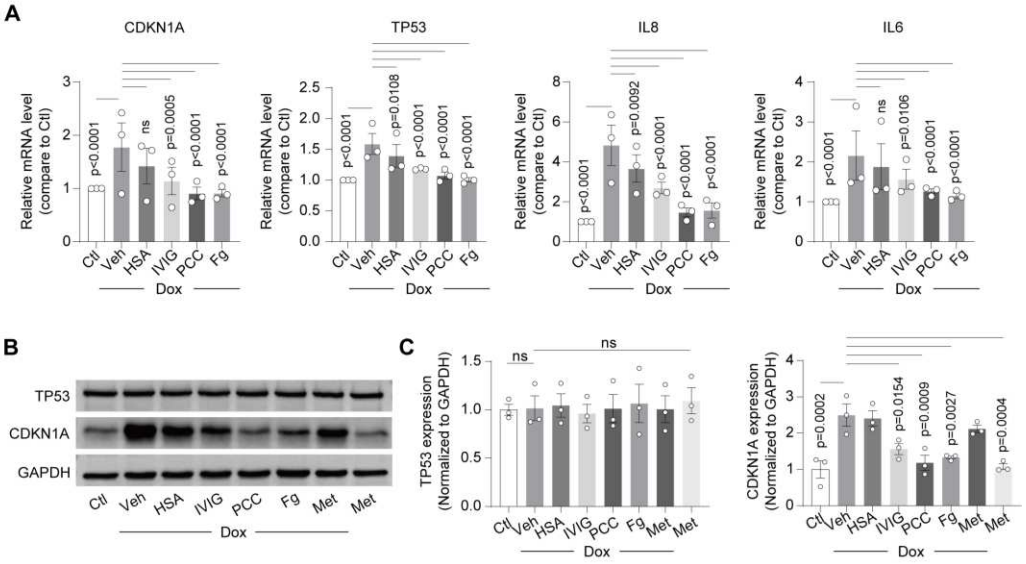
Figure 4. PCC and fibrinogen reduce doxorubicin-induced γH2AX foci burden in HUVECs. (A) Representative confocal images of γH2AX immunofluorescence in HUVECs treated with doxorubicin (Dox, 20 nM) in the absence or presence of HSA (2 mg/ml), IVIG (6.25 mg/ml), PCC (0.375 IU/ml), or Fg (3.75 mg/ml). Nuclei were counterstained with DAPI (blue), and γH2AX is shown in green. Merged images are shown. Scale bar, 50 μm. (B) Quantification of the average number of γH2AX foci per nucleus. Data are presented as mean ± SEM from six independent biological replicates, with six microscopic fields analyzed per replicate. Each biological replicate contributed one value to the statistical analysis. Statistical analysis was performed using one-way ANOVA followed by Tukey's multiple-comparison test. P values for significant pairwise comparisons are indicated in the figure.

628 **Figure 1**



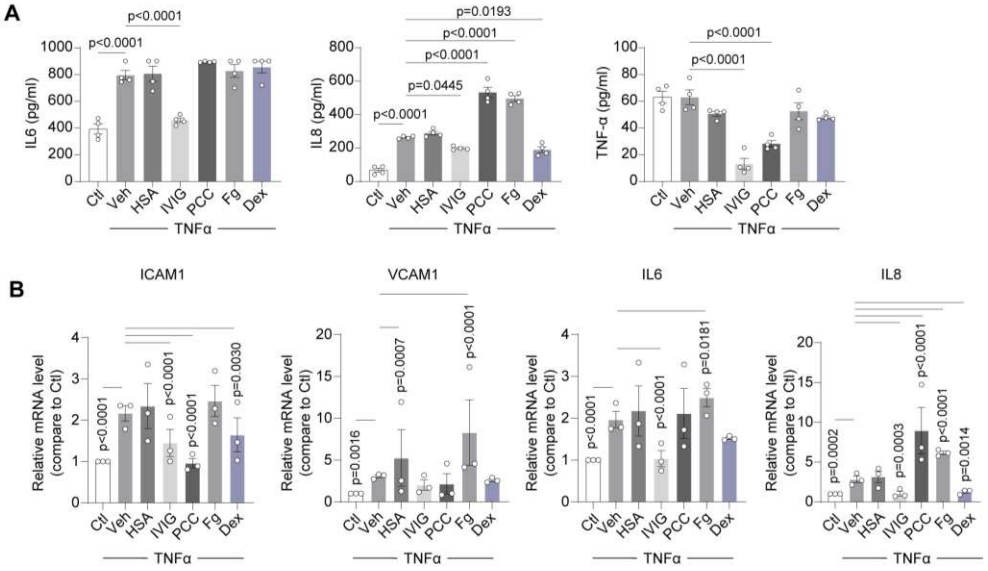
629
630

631 **Figure 2**

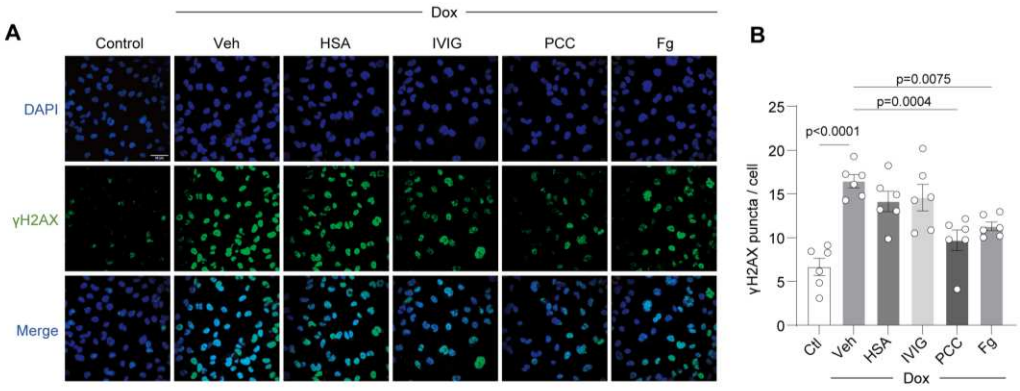


632
633

Figure 3


A
IL6 (pg/ml)
IL8 (pg/ml)
TNF-α (pg/ml)
Ctl
Veh
HSA
IVIG
PCC
Fg
Dex
TNFα
B
ICAM1
VCAM1
IL6
IL8
Relative mRNA level (compare to Ctl)

637 **Figure 4**



638
639

640 **Table 1. List of primer sequences used in the quantitative real-time PCR**

Gene	Forward	Reverse
GAPDH	GGAGCGAGATCCCTCCAAAAT	GGCTGTTGTCATACTTCTCATGG
ACTB	CATGTACGTTGCTATCCAGGC	CTCCTTAATGTCACGCACGAT
ICAM1	ATGCCCAGACATCTGTGTCC	GGGGTCTCTATGCCCAACAA
VCAM1	TTTGACAGGCTGGAGATAGACT	TCAATGTGTAATTTAGCTCGGCA
IL6	ACTCACCTCTTCAGAACGAATTG	CCATCTTTGGAAGGTTCAGGTTG
IL8	ACCCCAAGGAAAACTGGGTG	TGCTTGAAGTTTCACTGGCA
CDKN1A	CCTGGTGATGTCCGACCTG	CCATGAGCGCATCGCAATC
CDKN2A	CGCAGGTTCTTGGTCACTGT	TGTTCACGAAAGCCAGAGCG
TP53	GTCACAGCACATGACGGAGG	TCTTCCAGATGCTCGGGATAC

641

Supplementary Files

This is a list of supplementary files associated with this preprint. Click to download.

- SupplementalInformation.pdf